25th Australasian Conference on Mechanics of Structures and Materials (ACMSM25)
Edited by C.M. Wang, J.C.M. Ho and S. Kitipornchai
Brisbane, Australia, December 4 – 7, 2018

COUPLING FINITE ELEMENTS FOR MODELLING FLUID FLOW IN FRACTURED POROUS MEDIA

B. VAFAJOU[1], D. DIAS-DA-COSTA[1,2,*], L.A.G. BITENCOURT JR.[3] and O.L. MANZOLI[4]

[1]School of Civil Engineering, University of Sydney, NSW 2006, Australia

[2]ISISE, Department of Civil Engineering, University of Coimbra, Portugal

[3]Polytechnic School at the University of São Paulo, CEP 05508-010, São Paulo, Brazil

[4]São Paulo State University, UNESP/Bauru, CEP 17033-360, São Paulo, Brazil

Emails: behnam.vafajoudamirchi@sydney.edu.au, daniel.diasdacosta@sydney.edu.au, luis.bitencourt@usp.br, omanzoli@feb.unesp.br

*Corresponding author

Abstract. *The presence of discontinuities such as cracks and faults in porous media can remarkably affect the fluid pressure distribution. This is due to considerable contrast between hydraulic properties of porous matrix and discontinuity. Several numerical techniques have been adopted to simulate the behaviour of fractured porous media subjected to fluid flow mostly in the context of discrete fracture-matrix models. Current approaches still have several shortcomings, namely in terms of computational costs from large number of additional degrees of freedom to capture the discontinuities, and the implementation of special integration procedures. The present work proposes a new technique to model fluid flow in saturated fractured porous media based on coupling finite elements to enable embedding the preferential paths of flow created by discontinuities in regular meshes. The discretisation of fracture and porous medium does not need to conform and the meshes are coupled without additional degrees of freedom. Two numerical examples are presented to assess the performance of the new method in comparison with other techniques available in the literature.*

Keywords: Fractured porous media; Darcy's law; coupling finite elements.

1 INTRODUCTION

It is widely known that natural or engineered discontinuities such as joints, faults, planes, and human-induced fractures can strongly influence the fluid pressure distribution in porous media. In most cases, the discontinuities increase the permeability of the material and act as preferential flow paths. This can significantly impact the response of the system for example in management of groundwater resources. Three main groups of numerical models can be found in the literature for simulating fluid flow in fractured porous media. The first group is quite suitable for large scale problems since it is based on the replacement of the fractured medium by an equivalent continuum model with averaged properties (Jackson et al., 2000; Long et al., 1982). The second type of approach handles both porous medium and discontinuities using their own hydraulic properties, in what is known as a dual porosity model (Barenblatt et al., 1960; Moench, 1984; Zimmerman et al., 1993). Discrete-fracture matrix (DFM) methods compose the third group (Andersson and Dverstorp, 1987; Sudicky and McLaren, 1992; Woodbury and Zhang, 2001), in which individual discontinuities are considered explicitly with the flux exchange with the surrounding porous domain. Over the last decades, various DFM methods were

proposed for the discretisation of fractured porous media and these were gradually improved towards more realistic descriptions of the processes involved. Boone and Ingraffea (1990) developed a numerical strategy that combined the finite element method (FEM) – to model the mechanical deformation – with the finite difference method (FDM) – to capture the flow through the discontinuity. In such models, discontinuities and neighbouring porous domain are discretised using a hybrid-dimensional approach, i.e. the number of dimensions required by the fracture is one unit less than that of the surrounding matrix (Bogdanov et al., 2003; Helmig, 1997; Martin et al., 2005).

Classical DFM models rely heavily on matching grids for discontinuities and porous discretised domains. In order to overcome such mesh dependency, the extended finite element method (X-FEM) has been employed and several non-conforming DFM models were introduced in recent years (D'Angelo and Scotti, 2012; Flemisch et al., 2016; Huang et al., 2011; Schwenck et al., 2015). Unfortunately, such approach requires cumbersome integration procedures and significant number of additional degrees of freedom to capture the discontinuities. This can be quite prohibitive for general problems.

This paper proposes an innovative approach based on coupling finite elements (CFEs) to independently discretise both discontinuities and porous media. Even though both meshes are non-matching, there is no need for additional degrees of freedom (Bitencourt Jr. et al., 2015). The formulation is based on standard element shape functions to avoid particular integration procedures. The paper is organised as follows. Section 2 describes the governing equations for fluid flow in fractured porous media and discretisation procedure. The coupling elements are introduced in Section 3, whereas two case studies are analysed in Section 4. Finally the main conclusions are presented in Section 5.

2 GOVERNING EQUATIONS OF FLUID FLOW

2.1 Strong form

2.1.1 Flow in matrix

A 2-D fractured saturated porous medium with an incompressible single-phase fluid is considered in this paper – see schematic representation in Fig. 1.

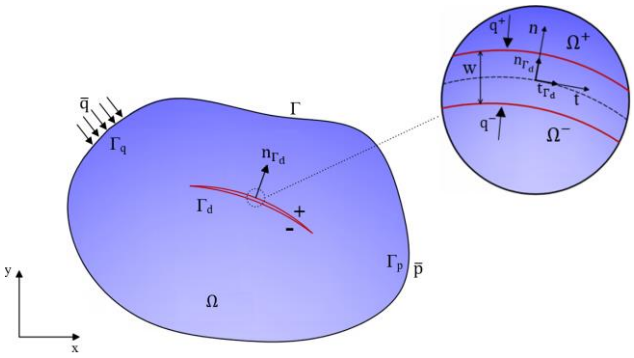

Figure 1: Domain and boundary conditions of a general fractured porous medium.

The continuity equation for the steady flow of an incompressible fluid phase over a fixed porous medium, Ω, in the absence of body forces and sinks (or sources) can be written as (Whitaker, 1966):

$$\nabla . v_m = 0. \tag{1}$$

The Darcy's law is applied to describe the flow in the porous matrix as:

$$v_m = -\frac{k_m}{\mu} \nabla p_m, \tag{2}$$

where v_m denotes the representative element volume fluid average velocity, whereas k_m, μ and p_m stand for the permeability, fluid viscosity and pressure, respectively. By inserting Eq. (2) into Eq. (1) the following standard form is obtained (Muskat, 1937):

$$\nabla . \left(\frac{k_m}{\mu} \nabla p_m\right) = 0. \tag{3}$$

The latter equation can be solved by imposing the boundary condition $p_m = \bar{p}$ on Γ_p and $q_m.n_\Gamma = \bar{q}$ on Γ_q, where q_m is the fluid flux, and $\Gamma = \Gamma_p \cup \Gamma_q$ is the boundary of the domain as represented in Fig. 1.

2.1.2 Flow in a discontinuity

The continuity equation for the steady state fluid flow along the discontinuity is given by (Segura and Carol, 2004):

$$-\frac{dq_d}{d\Gamma} + q^- + q^+ = 0, \tag{4}$$

where q_d is the longitudinal flow, q^- and q^+ are the fluxes incoming the discontinuity from the surrounding continuum medium, as shown in Fig. 1. The local flux at the discontinuity, q_l, and longitudinal flow are related with the crack width, w, by $q_d = w\, q_l$. Since the longitudinal flow can be considered steady, it can be approximated by Darcy's law as follows:

$$q_l = -\frac{k_l}{\mu} \frac{dp_d}{d\Gamma}, \tag{5}$$

where p_d is the fluid pressure. It is worth emphasising that the permeability of the discontinuity, k_l, highly depends on the crack width. In an ideal case where two parallel planes at constant distance are filled with porous material, e.g. the permeability can be obtained directly using the cubic law (Witherspoon et al., 1980):

$$k_l = \frac{1}{f}\frac{w^2}{12}, \tag{6}$$

where 'f' represents a correction coefficient typically in the range of 1.04 to 1.65 to account for situations other than the ideal (Adler et al., 2012).

By substituting Eq. (5) into (4), the following governing equation can be obtained:

$$\frac{d}{d\Gamma}\left(\frac{k_d}{\mu} \frac{dp_d}{d\Gamma}\right) + q^- + q^+ = 0, \tag{7}$$

where k_d stands for the permeability of the discontinuity, i.e., $k_d = w\, k_l$.

2.2 Weak form

The weak form of Eqs. (3) and (7) is derived, respectively, by multiplying the virtual quantities, δp_m and δp_d, both satisfying the essential boundary conditions, and integrating over domains Ω and Γ_d:

$$\int_\Omega \delta p_m \left[\nabla . \left(\frac{k_m}{\mu} \nabla p_m\right)\right] d\Omega = 0, \tag{8}$$

$$\int_{\Gamma_d} \delta p_d \left[\frac{d}{d\Gamma} \left(\frac{k_d}{\mu} \frac{dp_d}{d\Gamma} \right) + q^- + q^+ \right] d\Gamma = 0. \tag{9}$$

The above integral equations can be further developed using the Divergence theorem and integrating by parts, in which case the following governing equations are finally obtained:

$$- \int_{\Omega} \nabla \delta p_m \frac{k_m}{\mu} \nabla p_m d\Omega + \int_{\Gamma_q} \delta p_m (q_m . n_\Gamma) d\Gamma = 0, \tag{10}$$

$$- \int_{\Gamma_d} \left[\frac{d\, \delta p_d}{d\Gamma} \left(\frac{k_d}{\mu} \frac{dp_d}{d\Gamma} \right) \right] d\Gamma + \int_{\Gamma_{d^-}} \delta p_d \, q^- d\Gamma + \int_{\Gamma_{d^+}} \delta p_d \, q^+ d\Gamma = 0. \tag{11}$$

2.3 The FEM discretisation

Eqs. (10) and (11) are herein discretised with bidimensional elements for the porous domain and unidimensional elements for the discontinuities, as shown in Fig. 2. Accordingly, the pressure field in the porous domain is approximated by:

$$p_m = N_m \bar{p}_m, \tag{12}$$

and along the discontinuity by:

$$p_d = N_d \bar{p}_d, \tag{13}$$

where N_m, N_d , $\bar{p}_m$, $\bar{p}_d$ are the shape functions and nodal pressures for domain and discontinuity, respectively. By replacing Eqs. (12) and (13) in (10) and (11), respectively, the uncoupled finite element discretisation is finally written as:

$$H_m \, p_m = q_m, \tag{14}$$

$$H_d \, p_d = q_d, \tag{15}$$

where H_m, H_d are the permeability matrices for domain and discontinuity, respectively, defined by:

$$H_m = \int_{\Omega} B_m{}^T \frac{k_m}{\mu} B_m \, d\Omega, \tag{16}$$

$$H_d = \int_{\Gamma_d} B_d{}^T \frac{k_d}{\mu} B_d \, d\Gamma, \tag{17}$$

$$q_m = \int_{\Gamma_q} N_m{}^T \bar{q} \, d\Gamma, \tag{18}$$

$$q_d = \int_{\Gamma_{d^-}} N_d{}^T q^- d\Gamma + \int_{\Gamma_{d^+}} N_d{}^T q^+ \, d\Gamma, \tag{19}$$

in Eqs. (16) and (17), B_m and B_d stand for the partial derivatives of the shape functions of the element. It should be emphasised that the discretisation shown in Eqs. (14) and (15) is carried out independently, with the connection between the meshes being established after this step using coupling finite elements. This procedure is addressed in the next section.

3 CFE FORMULATION

For a typical finite element with ‘n’ nodes, the fluid pressure at any point inside its domain can be approximated by:

$$p_m = \sum \bar{N}_i \, \bar{p}_i \,, \tag{20}$$

where $\bar{N}_i$ and $\bar{p}_i$ are, respectively, the shape function and nodal pressure for node ‘i’. If the element is crossed by a discontinuity, then a coupling element exactly matching the underlying element and having an additional node, n+1, herein designated by C_{node}, overlaps the standard element. The additional node is used to connect the finite element for the porous medium with the discontinuity inside its domain. It should be highlighted that the additional node will not require more degrees of freedom in the global system of equations and it can also be located anywhere inside the element, including along its boundaries, as shown in Fig. 2. In this figure, two coupling elements, both with an additional node, are used to establish the connection with the two nodes that define the discontinuity: element e_i matches the standard bilinear element on midlle and contains the coupling node C_{node_i}; and element e_j matches the standard element on the right and contains the second coupling node C_{node_j}.

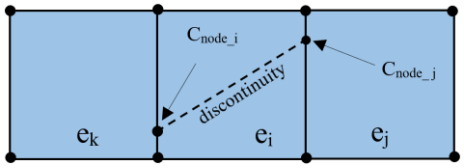

Figure 2: Illustration of two CFEs used to couple the underlying mesh with the discontinuity.

To establish the connection between the meshes, the pressure drop between the coupling node, C_{node}, and the material point inside the standard element at the same location, X_c, has to be zero. Using the standard shape function, the following can be written:

$$[\![P]\!] = p_{n+1} - \bar{p}\,(X_c) = p_{n+1} - \sum_{i=1}^{n} \bar{N}_i\,(X_c)\, p_i = N_e\, P_e \,, \tag{21}$$

where matrices N_e and P_e are given by:

$$N_e = [-\bar{N}_1(X_c) \;\; -\bar{N}_2(X_c) \ldots \;\; -\bar{N}_n(X_c) \;\; 1] \text{ and} \tag{22}$$

$$P_e = [p_1 \;\; p_2 \cdots p_n \;\; p_{n+1}]^T. \tag{23}$$

Following the analogy between mechanical and hydraulic problems discussed in (Segura and Carol, 2004), an equivalent internal virtual work, δW^{int} for the CFE is obtained as:

$$\delta W^{int} = \delta[\![P]\!]\; q([\![P]\!]) \,, \tag{24}$$

where q is the flux associated with the pressure drop and the virtual pressure drop is given by:

$$\delta[\![P]\!] = N_e \; \delta P_e \,. \tag{25}$$

Since the internal flow input is expressed by:

$$q^{int} = N_e{}^T q\,([\![P]\!]), \tag{26}$$

the tangent stiffness matrix of the CFE is obtained by $K_e = \partial q^{int} / \partial P_e$, i.e.:

$$K_e = N_e{}^T \, C \, N_e, \tag{27}$$

where $C = \partial q[\![P]\!] / \partial [\![P]\!]$.

It is herein assumed a linear relation between the pressure drop and flux, in which case C is a constant penalty factor enforcing a null pressure drop, i.e. the compatibility between meshes.

4 CASE STUDIES

In the following sections two case studies are presented to validate the CFEs, the first with a single and the second with multiple discontinuities. Bilinear elements are used to discretise the porous domain and linear elements are adopted for the discontinuities, whereas CFEs establish the connection between the sets of meshes.

4.1 Porous medium with a single discontinuity

The first verification example consists of a 2-D rectangular domain with 10 m by 16 m. A pressure difference of 286 kPa is applied between bottom and top, and no flow is allowed through the sides. The permeability of the porous matrix is 8 mD (millidarcy), i.e. 7.896×10^{-15} m^2. A discontinuity is defined with 45° inclination relatively to boundaries and through the centre. Its permeability is 80 D (Darcy), i.e. 7.896×10^{-11} m^2 – see Figure 3.a. Results obtained by Lamb (2011) using a discrete fracture model (DFM), a mesh-free model (FM-Mfree), and a finite element method (FM-FEM), and by Liu et al. (2015) using X-FEM, are used for validation.

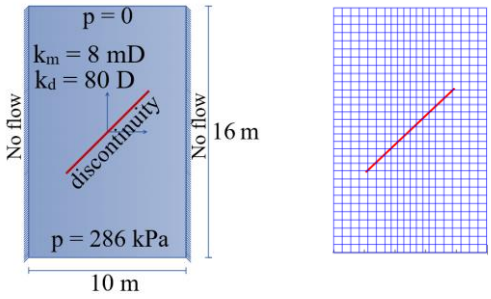

(a) (b)

Figure 3: Fractured porous medium: (a) geometry and boundary conditions; (b) FEM mesh.

Figure 3.b shows the mesh adopted, which has the same number of bilinear elements as in the X-FEM example mentioned above. In total 620 bilinear elements, 26 linear elements, and 27 coupling elements are used. It can already be highlighted that even though the standard bilinear elements adopted by X-FEM and the model with CFEs are indeed the same, the former formulation requires 62 additional degrees of freedom to discretise the crack, whereas only 27 are used in the present formulation.

Figs. 4 and 5a depict the pressure distribution inside the domain, and the profile along a vertical section through the centre. From the represented values, it can be concluded that the mesh with CFEs provides accurate results, with the pressure distribution properly reflecting the impact of the discontinuity. It should be mentioned that both meshes are non-conforming conversely to all other models used for comparison. In addition, Fig. 5b shows the change in pressure at the centre of the discontinuity for different values of the coupling stiffness. The results are very stable and insensitive to the parameter for the tested range.

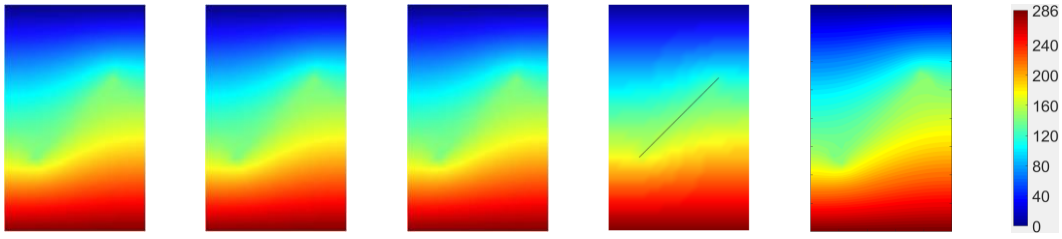

(a) DFM (Lamb, 2011) (b) FM-FEM (Lamb, 2011) (c) FM-MFree (Lamb, 2011) (d) X-FEM (Liu et al. 2015) (e) CFEs (this study)

Figure 4: Pressure field obtained with different methods.

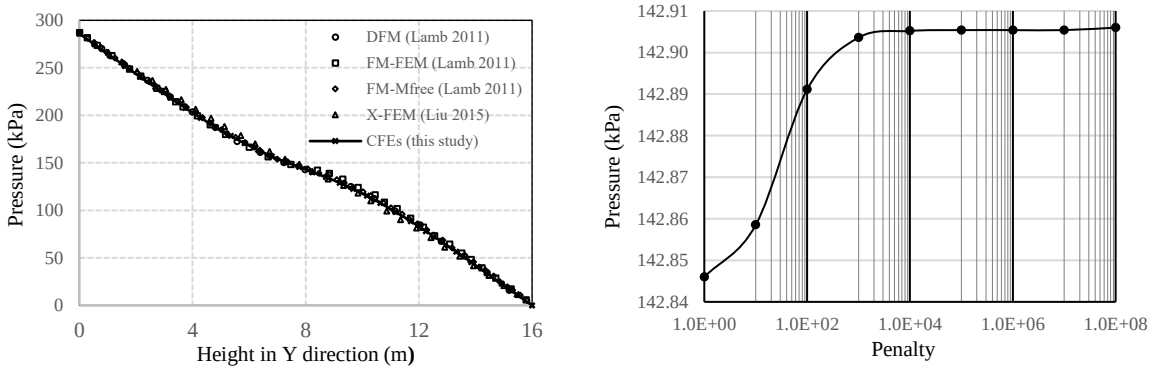

(a) (b)

Figure 5: Pressure (a) along a vertical section across the centre of the domain; and (b) at the midpoint of the discontinuity versus coupling stiffness.

4.2 Dam foundation with multiple discontinuities

The example shown in Fig. 6.a is based on the study presented by Segura and Carol (2004) on a dam foundation with multiple discontinuities. The soil underneath the gravity dam has an hydraulic conductivity (hc) of 10^{-7} m/s, and three longitudinal conductivities are used for each model containing the discontinuities: 8.1182×10^{-10}, 1.0148×10^{-7}, 8.1182×10^{-7} m^2/s.

Figure 6.b compares the pressure obtained for each value of the conductivity using the model with CFEs in comparison with benchmark results obtained using zero-thickness interface elements (Segura and Carol, 2004). The proposed formulation provides nearly the same results even though the meshes are non-conforming and use substantially less degrees of freedom. With increasing longitudinal hydraulic conductivity, the fluid flows easier through the discontinuities thus leading to higher values of hydraulic head, particularly in the region directly underneath the dam .

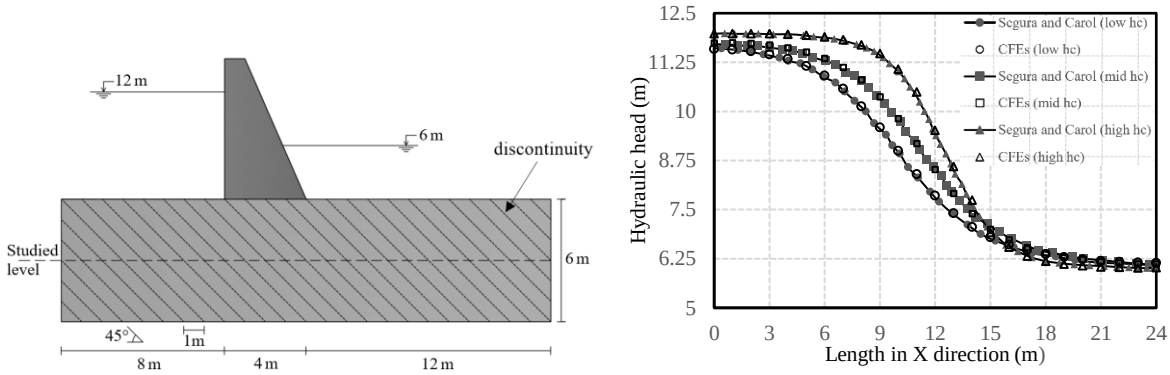

(a) (b)

Figure 6: (a) Geometry and boundary conditions; and (b) pressure distribution along the studied level.

5 CONCLUSIONS

A new technique based on CFEs was proposed in this paper to couple non-conforming meshes in steady state flow problems. The discretisation can be carried out independently for discontinuities and porous medium, and without additional degrees of freedom to establish the connection between the two. The bidimensional examples shown the ability to handle single and multiple discontinuities against several existing methods, including X-FEM and zero-thickness interface elements. The obtained results were not sensitive to the coupling stiffness. Given the advantages found, namely in the simplification of

the meshing process together with the possibility of using standard shape functions and integration procedures, the formulation will be further developed to deal with more general examples including the transverse pressure drop across discontinuities.

ACKNOWLEDGMENTS

The authors would like to acknowledge the support from the Australian Research Council through its Discovery Early Career Researcher Award (DE150101703) and ARC Projects (DP170104192, LP140100591), and from the School of Civil Engineering at The University of Sydney. The third and fourth authors would also to acknowledge the support from the Petrobras S/A.

REFERENCES

Adler, P. M., Thovert, J.-F., and Mourzenko, V. V. (2012). Fractured porous media, Oxford University Press, Oxford, UK, 175pp.

Andersson, J., and Dverstorp, B. (1987). Conditional simulations of fluid flow in three-dimensional networks of discrete fractures. Water Resources Research, 23(10), 1876-1886.

Barenblatt, G., Zheltov, I. P., and Kochina, I. (1960). Basic concepts in the theory of seepage of homogeneous liquids in fissured rocks [strata]. Journal of applied mathematics and mechanics, 24(5), 1286-1303.

Bitencourt Jr., L. A. G., Manzoli, O. L., Prazeres, P. G., Rodrigues, E. A., and Bittencourt, T. N. (2015). A coupling technique for non-matching finite element meshes. Computer methods in applied mechanics and engineering, 290, 19-44.

Bogdanov, I., Mourzenko, V., Thovert, J.-F., and Adler, P. (2003). Two-phase flow through fractured porous media. Physical Review E, 68(2), 1-24.

Boone, T. J., and Ingraffea, A. R. (1990). A numerical procedure for simulation of hydraulically-driven fracture propagation in poroelastic media. International Journal for Numerical and Analytical Methods in Geomechanics, 14(1), 27-47.

D'Angelo, C., and Scotti, A. (2012). A mixed finite element method for Darcy flow in fractured porous media with non-matching grids. ESAIM: Mathematical Modelling and Numerical Analysis, 46(2), 465-489.

Flemisch, B., Fumagalli, A., and Scotti, A. (2016). A review of the XFEM-based approximation of flow in fractured porous media, Advances in Discretization Methods, 47-76.

Helmig, R. (1997). Multiphase flow and transport processes in the subsurface: a contribution to the modeling of hydrosystems, Springer-Verlag Berlin Heidelberg, Berlin, Germany, 367pp.

Huang, H., Long, T. A., Wan, J., and Brown, W. P. (2011). On the use of enriched finite element method to model subsurface features in porous media flow problems. Computational Geosciences, 15(4), 721-736.

Jackson, C. P., Hoch, A. R., and Todman, S. (2000). Self consistency of a heterogeneous continuum porous medium representation of a fractured medium. Water Resources Research, 36(1), 189-202.

Lamb, A. R. (2011). Coupled deformation, fluid flow and fracture propagation in porous media, PhD Thesis, Department of Earth Science and Engineering, Imperial College, UK, 197pp.

Liu, F., Zhao, L.-Q., Liu, P.-L., Luo, Z.-F., Li, N.-Y., and Wang, P.-S. (2015). An extended finite element model for fluid flow in fractured porous media. Mathematical Problems in Engineering, 2015, 1–10.

Long, J., Remer, J., Wilson, C., and Witherspoon, P. (1982). Porous media equivalents for networks of discontinuous fractures. Water Resources Research, 18(3), 645-658.

Martin, V., Jaffré, J., and Roberts, J. E. (2005). Modeling fractures and barriers as interfaces for flow in porous media. SIAM Journal on Scientific Computing, 26(5), 1667-1691.

Moench, A. F. (1984). Double-porosity models for a fissured groundwater reservoir with fracture skin. Water Resources Research, 20(7), 831-846.

Muskat, M. (1937). The flow of fluids through porous media. Journal of Applied Physics, 8(4), 274-282.

Schwenck, N., Flemisch, B., Helmig, R., and Wohlmuth, B. I. (2015). Dimensionally reduced flow models in fractured porous media: crossings and boundaries. Computational Geosciences, 19(6), 1219-1230.

Segura, J., and Carol, I. (2004). On zero-thickness interface elements for diffusion problems. International journal for numerical and analytical methods in geomechanics, 28(9), 947-962.

Sudicky, E., and McLaren, R. (1992). The Laplace transform Galerkin technique for large-scale simulation of mass transport in discretely fractured porous formations. Water Resources Research, 28(2), 499-514.

Whitaker, S. (1966). The equations of motion in porous media. Chemical Engineering Science, 21(3), 291-300.

Witherspoon, P. A., Wang, J. S., Iwai, K., and Gale, J. E. (1980). Validity of cubic law for fluid flow in a deformable rock fracture. Water Resources Research, 16(6), 1016-1024.

Woodbury, A., and Zhang, K. (2001). Lanczos method for the solution of groundwater flow in discretely fractured porous media. Advances in Water Resources, 24(6), 621-630.

Zimmerman, R. W., Chen, G., Hadgu, T., and Bodvarsson, G. S. (1993). A numerical dual-porosity model with semianalytical treatment of fracture/matrix flow. Water Resources Research, 29(7), 2127-2137.